Available online at www.sciencedirect.com
ScienceDirect
Journal of Catalysis 248 (2007) 249–257
JOURNAL OF CATALYSIS
www.elsevier.com/locate/jcat

Evaluation of deactivation mechanisms of Pd-catalyzed hydrogenation of *4*-isobutylacetophenone

Nakul Thakar *, Tilman J. Schildhauer, Wim Buijs, Freek Kapteijn, Jacob A. Moulijn

Catalysis Engineering, DelftChemTech, Delft University of Technology, Julianalaan 136, 2628 BL, Delft, The Netherlands

Received 4 December 2006; revised 12 March 2007; accepted 13 March 2007

Available online 27 April 2007

Abstract

Pd catalysts were investigated for the hydrogenation of *4*-isobutylacetophenone (*4*-IBAP) and for Pd/SiO_2 an improved (compared with the non-patented literature) yield of nearly 80% of the desired product *1*-(*4*-isobutylphenyl)ethanol (*4*-IBPE) was obtained. However, severe catalyst deactivation was observed. The spent catalyst was characterized using a wide variety of thermal (TGA, TPO-MS), microscopic (TEM), and spectroscopic (DRIFT, LEIS) characterization techniques. Pd leaching did not occur. Oligomerization of *4*-IBAP by condensation reactions due to the acidity imparted by the presence of isolated silanol groups on SiO_2 is proposed as one of the causes of catalyst deactivation. Pd crystallite growth and strong chemisorption of the H_2O liberated by *4*-IBPE hydrogenolysis also contributed to the loss of catalytic activity. The conclusions are supported by the high stability of Pd black in catalyzing the reaction.

Keywords: Pd catalysts; Aryl ketone hydrogenation; Catalyst deactivation; LEIS

1. Introduction

The liquid-phase hydrogenation of *4*-isobutylacetophenone (*4*-IBAP) (Scheme 1) using supported noble metal catalysts is a step in the new catalytic route developed by Hoechst–Celanese [1] for the synthesis of ibuprofen, a nonsteroidal anti-inflammatory drug. The secondary alcohol derivative, *1*-(*4*-isobutylphenyl)ethanol (*4*-IBPE) is the product of interest in this case. The *4*-IBPE is further carbonylated to yield ibuprofen. Most of the earlier work on *4*-IBAP hydrogenation is patented, and only a few publications deal with the reaction mechanism and selectivity issues. The existing literature on the hydrogenation of *4*-IBAP is presented in Table 1 [2]. The Hoechst–Celanese patent [1] focuses on the carbonylation step for the synthesis of ibuprofen, and the hydrogenation step is only mentioned in one example; for this step, a large quantity of Pd/C catalyst is used (*4*-IBAP: 5% Pd/C in a weight ratio of 7:1). The knowledge provided by the patents is very limited and general in nature. The hydrogenation of *4*-IBAP using Ru/Al_2O_3 and Ni/HY has been investigated in detail [2,3], and the kinetics for these catalysts have been determined. In general, it is observed that the use of high hydrogen partial pressures and a co-catalyst system are desirable for obtaining a high selectivity to the desired *4*-IBPE. The use of a supported Pd catalyst is preferred, because Pd is well known to selectively hydrogenate the carbonyl functional group of an aromatic ketone at relatively mild conditions to the hydroxyl group [4]. Consequently, Pd was tested over various supports, including SiO_2, C, and $CaCO_3$, with the aim of maximizing the yield of the desired product *4*-IBPE.

Deactivation of noble metal catalysts is quite common in the bulk chemicals industry and has been well documented [5,6]. Loss of catalytic activity due to coke formation is well known for fluidized catalytic cracking (FCC), oxidative dehydrogenation, and reforming processes [7]. Albers et al. [8] reviewed the poisoning and deactivation of supported palladium catalysts and concluded that the nature of the carbonaceous deposits and the strength of their interactions with surface sites of palladium catalysts are crucial with respect to a detrimental impact on activity. Only a few reports exist on catalyst deactivation in the much more complex fine chemical industry [9]. Although no mention has been made of cat-

* Corresponding author. Fax: +31 (0) 15 2785006.
E-mail address: n.thakar@tudelft.nl (N. Thakar).

0021-9517/$ – see front matter
doi:10.1016/j.jcat.2007.03.019

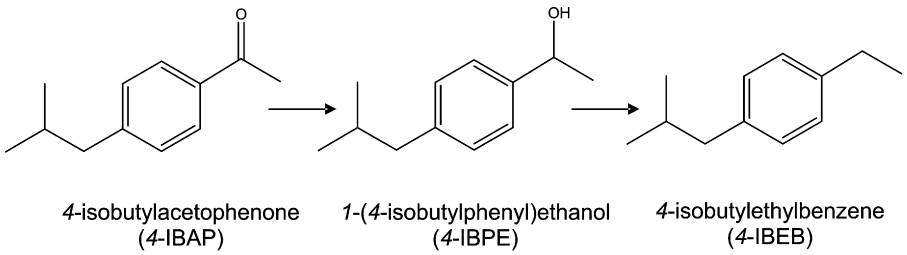

Scheme 1. Reaction scheme for *4*-IBAP hydrogenation.

Table 1
Literature review on *4*-IBAP hydrogenation

Catalyst	Promoter	Solvent	T (K)	p_{H_2} (MPa)	Conversion *4*-IBAP (%)	Selectivity *4*-IBPE (%)	Ref.
Pd/C	–	MeOH	303	6.8	99	97	[1]
Pd/C	Triethyl amine	MeOH	335	8.16	97	100	[10]
Pd/C	Aq. NaOH	*n*-Hexane	373	10.5	99	97	[1]
10% Ni/HY	NaOH	MeOH	373–393	3.0	75	75	[3]
2% Ru/Al_2O_3	–	MeOH	373–398	3.4–6.2	76	60	[2]
10% Ni, 1% Pt/HY	NaOH	MeOH	373	3.0	95	65	[13]

alyst deactivation problems in the existing patents on *4*-IBAP hydrogenation [10–12], Rajashekharam et al. [13] observed a significant decrease in activity on catalyst reuse for the hydrogenation of *4*-IBAP using Ni/HY catalyst. These authors proposed the use of a bimetallic Ni–Pt/HY catalyst that gave a slightly improved stability on reuse but did not evaluate the cause of catalyst deactivation. Although we achieved a relatively high yield (∼80%) of the desired product *4*-IBPE using a Pd/SiO_2 catalyst in a nonpolar solvent compared with that reported in the literature [2,3], the catalyst system was not satisfactory due to the severe catalyst deactivation observed. Because there is not much insight into the catalyst deactivation features for this important reaction (and other members of the class of aromatic ketones), this prompted us to investigate the catalyst deactivation for *4*-IBAP hydrogenation over Pd/SiO_2. Five theoretically possible reasons for catalyst deactivation suggest themselves: (i) the presence of strongly adsorbing impurities in the commercially available SiO_2 support or reactants; (ii) polymerization of the *4*-isobutylstyrene intermediate possibly formed during the transformation of *4*-IBPE to *4*-IBEB; (iii) strong adsorption of H_2O liberated during the transformation of *4*-IBPE to *4*-IBEB; (iv) Pd crystallite growth; and (v) oligomerization of *4*-IBAP or *4*-IBPE by condensation-type reactions. In this work, we analyze the possible contribution of each of the aforementioned phenomena toward catalyst deactivation.

2. Experimental

2.1. Materials and catalyst preparation

4-IBAP was purchased from Alfa Aesar. *n*-Decane and *n*-hexadecane were purchased from Aldrich. All of the chemicals were used as delivered without further purification. The *n*-decane and cyclohexane were used as nonpolar solvents, methanol was used as a polar solvent, and *n*-hexadecane was used as an internal standard. The 5 wt% Pd/C, 5 wt% $Pd/CaCO_3$, and Pd black are commercially available catalysts.

A series of Pd/SiO_2 catalysts were prepared by the wet-impregnation technique. Palladium acetate trimer purchased from Alfa Aesar was used as the palladium precursor, and Davisil 643 (35–74 μm) was used as the SiO_2 support. In a typical procedure to prepare the Pd/SiO_2 catalyst, the required amount of precursor was dissolved in an excess of toluene and added dropwise to the required amount of SiO_2 support suspended in toluene with continuous mixing. The mixing was carried out overnight. The catalyst was filtered from toluene under vacuum and dried in an oven at 373 K for 16 h. It was subsequently heated to 673 K at a rate of 0.5 K/min and calcined in air at 673 K for 5 h.

2.2. Catalyst characterization

2.2.1. Volumetric N_2 physisorption

N_2 physisorption experiments were performed at 77 K on a Quantachrome Autosorb 6B apparatus after degassing in vacuum at 423 K for 16 h. The amount of sample used was 0.1 g for the fresh catalyst and 0.05 g for the spent catalyst sample. The specific surface area of the samples was determined from the adsorption isotherms by the BET method.

2.2.2. CO chemisorption

The catalyst samples (0.1 g for the fresh catalyst and 0.05 g for the spent catalyst sample) were first dried in vacuum at 403 K (this dry sample weight was used in the calculations). Subsequently, the samples were reduced (100% H_2, 50 cm^3/min, 2 h) at 373 K, followed by evacuation (2 h) at 403 K. The adsorption measurements were performed at 313 K using CO as an adsorbate and assuming a CO:Pd = 1:1 stoichiometric ratio. Both the in situ pretreatment and the analysis were performed on a Quantachrome Autosorb-1C device.

2.2.3. Inductively coupled plasma-optical emission spectroscopy

Inductively coupled plasma-optical emission spectroscopy (ICP-OES) of the in-house-prepared Pd/SiO_2 catalysts was performed in a Perkin–Elmer Plasma 2000 apparatus to determine the Pd loading. For the analysis, the samples (0.05 g) were dried at 413 K for 5 h and then dissolved in a 1% HF and 1.3% H_2SO_4 solution.

2.2.4. Transmission electron microscopy

Transmission electron microscopy (TEM) was performed using a Philips CM30T electron microscope with a LaB_6 filament as the source of electrons operated at 300 kV. The reduced samples were mounted on Quantifoil microgrid carbon polymer supported on a copper grid by placing a few droplets of a suspension of the ground sample in hexane on the grid, followed by drying at ambient conditions.

2.2.5. Thermogravimetric analysis

Thermal analysis was performed on a TGA/SDTA851^e thermobalance from Mettler Toledo using approximately 0.02 g of sample. In the presence of flowing air (100 cm^3/min), the thermogravimetric (TG) and differential thermogravimetric (DTG) burn-off profiles of the spent catalyst sample were measured at a heating rate of 10 K/min from 298 to 1073 K.

2.2.6. Temperature-programmed oxidation-mass spectrometry

Temperature-programmed oxidation-mass spectrometry (TPO-MS) measurements were performed in a conventional flow apparatus using a quartz microreactor and He as a carrier gas flowing at 50 cc/min. About 0.1 g of the sample was heated at a rate of 10 K/min from 298 to 1173 K. The gaseous species from the sample were monitored by a prisma quadrupole mass spectrometer (Balzers) connected online with the reactor. Mass spectra were recorded in multiple ion detection (MID) mode using a channeltron detector. The evolved CO_2 and CO were calibrated following a method described by Wang and McEnaney [14] using thermal decompositions of calcium carbonate and calcium oxalate. A 10% correction for the fragmentation of CO_2 to CO was determined by this method, which was close to the 11% correction claimed by the equipment manufacturer.

2.2.7. Diffuse reflectance infrared Fourier transform spectrometry

Diffuse reflectance infrared Fourier transform spectrometry (DRIFTS) spectra for the fresh and spent Pd/SiO_2 samples were recorded on a single-beam Nicolet Magna 550 FTIR spectrometer in a Spectratech DRIFT accessory, against a background spectrum recorded for a sample cup filled with KBr. The spectra were obtained by collecting 256 scans at 8 cm^{-1} resolution and displayed in absorption reflectance units.

2.2.8. Low-energy ion scattering

Low-energy ion scattering (LEIS) experiments were performed in the ultra-high-vacuum LEIS instrument, which had a base pressure in the low 10^{-10} mbar range. The pressure increased to 10^{-9}–10^{-8} mbar during LEIS experiments due to noble gas influx from the ion source. The primary ions were mass selected, focused, and directed perpendicularly to the target. Ions scattered through 145° are accepted by the analyzer. The double-toroidal electrostatic analyzer makes very efficient use of the backscattered particles by measuring a continuous part of the energy spectrum of the backscattered particles and 320° of the azimuthal range simultaneously. The ion beam was rastered over an area of 2×2 mm^2 during the measurements, thus further reducing the ion-induced damage. The catalyst samples were mildly compacted by manually pressing a pestle on a sample holder filled with powder. $^4He^+$ and Ne^+ (useful for identifying heavier atoms) measurements were performed on 2×2 mm^2 areas of the fresh Pd/SiO_2 sample and of the SiO_2 support itself. Two spent catalyst samples were also analyzed: (i) Pd/SiO_2 held at reaction temperature for 12 h in a mixture of reactant and solvent under a N_2 atmosphere under stirring (spent Pd/SiO_2, N_2) and (ii) Pd/SiO_2 held at reaction temperature for 12 h in reactant and solvent, followed by a hydrogenation run for 5 h (spent Pd/SiO_2, H_2). Because it is not possible to differentiate between carbon present in the product/solvent and that present in the oligomers by the LEIS technique, the catalyst samples spent Pd/SiO_2, H_2 and spent Pd/SiO_2, N_2 were calcined in static air at 503 K to burn off any traces of product or solvent before LEIS measurements.

2.3. Hydrogenations

Catalytic hydrogenation of *4*-IBAP was carried out in a Premex 500-mL stainless steel stirred reactor equipped with a gas-induced stirrer. In a typical hydrogenation experiment, the catalyst was reduced in situ at 373 K for 1 h under 10 bar hydrogen pressure. After cooling, depressurizing, and flushing the reactor with N_2, the desired amounts of reactant (*4*-IBAP), solvent (*n*-decane), and internal standard (*n*-hexadecane) were charged to the reactor from the liquid holding vessel. The contents (∼200 mL) were flushed with nitrogen three times at room temperature. After the desired reaction temperature was attained, the system was pressurized with hydrogen to the required pressure. The reaction was started by switching on the stirrer; this was taken as time $t = 0$. The progress of the reaction was determined by monitoring the hydrogen supply rate (keeping the reactor pressure constant) as a function of time. Most semibatch experiments were carried out at standard conditions of 373 K and 2.0 MPa H_2 pressure in *n*-decane using 0.1 g of catalyst and a stirring speed of 1500 rpm. After the completion of the reaction, as indicated by no further hydrogen consumption, the reactor was cooled to room temperature and depressurized prudently. In all experiments, concentration–time data were generated by intermediate sampling of the liquid phase (∼250 μL) and sample analysis by gas chromatography (Chrompack CP9001 equipped with an autosampler), which was fitted with a CP Sil 8 CB column (50 m × 0.25 mm). The conditions were as follows: FID temperature, 523 K; injector temperature, 523 K; column temperature increased linearly from 323 to 523 K at a rate of 6.7 K/min.

Table 2
Metal loading of catalysts and corresponding surface areas

Catalyst	Active metal surface area (m^2/g_{cat})	Average Pd crystal size (nm)	Pd dispersion (%)
0.8% Pd/SiO_2[b]	1.4	3.6	30
2.4% Pd/SiO_2[b]	3.4	3.5	32
5% Pd/C[a]	7.4	3.4	33
5% $Pd/CaCO_3$[a]	1.4	17.5	6
Pd black[a]	6.7	74	1.5

[a] Commercial catalyst.
[b] Pd loading determined by ICP.

3. Results

Table 2 gives the actual Pd loadings, along with the active metal surface areas of the various catalysts used. Fig. 1 compares the initial activity at 20% *4*-IBAP conversion for a 2.4 wt% Pd/SiO_2 catalyst in polar and nonpolar solvents. The highest initial activity ($mol_{IBAP}/kg_{Pd}/s$) was observed for a nonpolar solvent (*n*-decane), which was then used as the solvent of choice for all further reactions. The in-house-prepared 2.4 wt% Pd/SiO_2 catalyst performed at least as good as the commercial 5 wt% Pd/C catalyst (Fig. 2), based on the initial activity normalized with respect to the active metal surface area ($mmol_{IBAP}/m^2_{Pd}/s$) for a fair comparison between catalysts of different loadings. The 2.4 wt% Pd/SiO_2 showed relatively high activity and full conversion in a reasonable time period and thus was used for all further experiments. Reference to Pd/SiO_2 hereinafter implies a 2.4 wt% Pd loading unless specified otherwise.

Only two major products were observed in GC analysis, identified as *1*-(*4*-isobutylphenyl)ethanol (*4*-IBPE) and *4*-isobutylethylbenzene (*4*-IBEB) using GC-MS. A similar reaction profile was observed on using Pd black. This suggests that the transformation of *4*-IBPE to *4*-IBEB occurs via direct hydrogenolysis on the metal surface. Conclusive evidence of the hydrogenolysis pathway and the absence of the *4*-isobutylstyrene intermediate was obtained by deuteration studies [15]. The reaction scheme for *4*-IBAP hydrogenation is shown in Scheme 1. To confirm the absence of Pd leaching into the reaction mixture, the reaction was carried out up to 50% conversion (Fig. 3a) followed by hot filtration. The filtered reaction mixture was reheated to the reaction temperature ($T = 373$ K), pressurized with hydrogen, and stirred for 50 min. No further reaction occurred, as indicated by the absence of H_2 consumption. When fresh catalyst was added (Fig. 3b), the reaction proceeded further to completion, confirming the absence of significant Pd leaching into the solution. This result was also supported by ICP analysis of the reaction mixture, which showed no significant Pd in the liquid reaction mixture ($<0.5\ mg_{Pd}/kg_{soln}$.)

The H_2O liberated during the transformation of *4*-IBPE to *4*-IBEB had an inhibiting effect. The activity reduced by 5- to 6-fold on the addition of 15 wt% H_2O (with respect to the reactant *4*-IBAP) [16]. Fig. 4a shows the performance of Pd/SiO_2 for the hydrogenation of *4*-IBAP using 0.1 g of catalyst. A yield (selectivity × conversion) of nearly 80% to *4*-IBPE was observed,

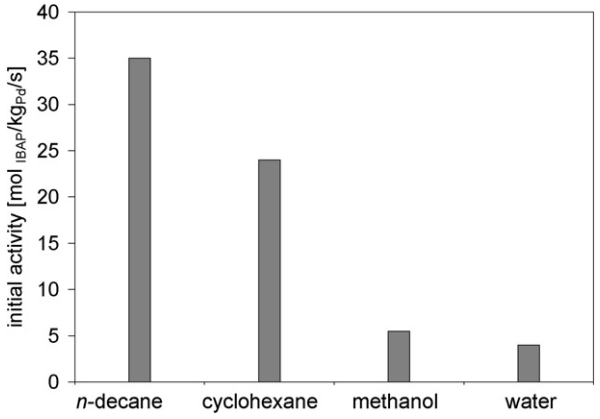

Fig. 1. Initial activity of 2.4% Pd/SiO_2 for *4*-IBAP hydrogenation in different solvents at standard conditions. Reaction conditions: $w_{cat} = 0.1$ g, $C_{IBAP} = 0.27$ mol/L, $T = 373$ K, $P_{H_2} = 2.0$ MPa, stirring rate = 1500 rpm.

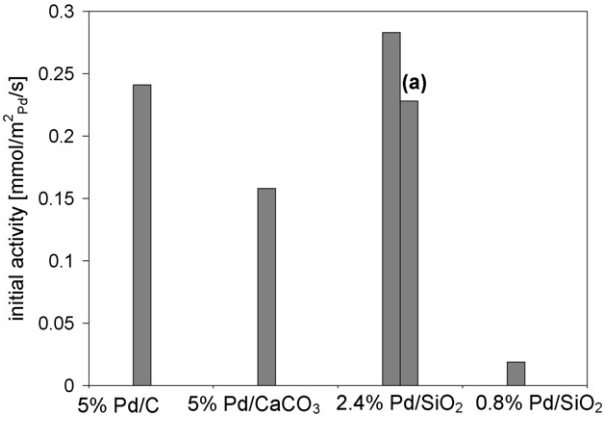

Fig. 2. Initial activity of different catalysts for *4*-IBAP hydrogenation under standard conditions. (a) Reaction started after overnight heating under inert atmosphere. Reaction conditions: $w_{cat} = 0.1$ g, $C_{IBAP} = 0.27$ mol/L, $T = 373$ K, $P_{H_2} = 2.0$ MPa, solvent *n*-decane, stirring rate = 1500 rpm.

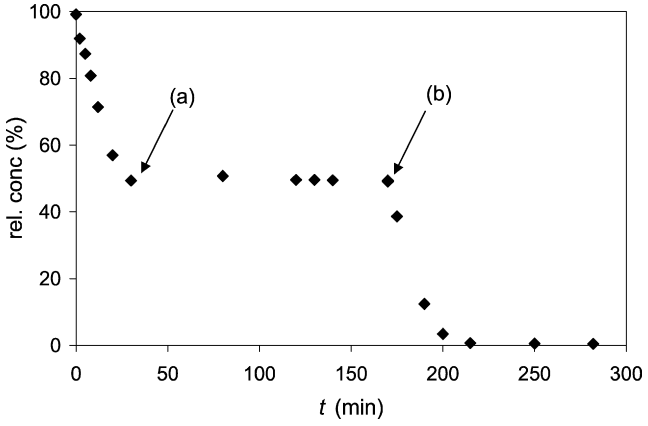

Fig. 3. Relative *4*-IBAP concentration versus time in a hydrogenation experiment. Reaction conditions: $w_{cat} = 0.1$ g, $C_{IBAP} = 0.27$ mol/L, solvent *n*-decane, $T = 373$ K, $P_{H_2} = 2.0$ MPa, stirring rate = 1500 rpm. (a) H_2 supply stopped and catalyst filtered off; (b) addition of 0.1 g fresh catalyst.

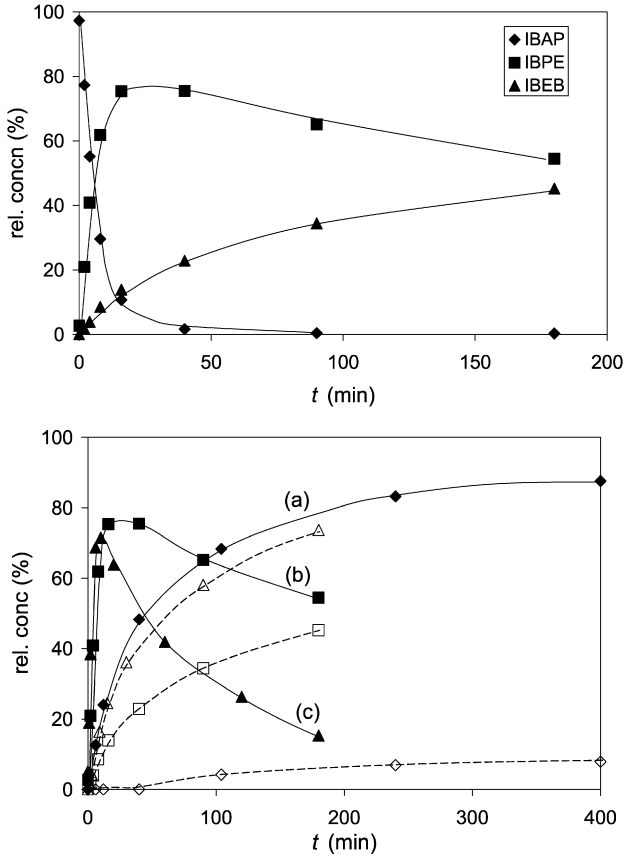

Fig. 4. (a) Relative concentration profiles during *4*-IBAP hydrogenation with Pd/SiO_2 as a function of reaction time under standard reaction conditions. Reaction conditions: $w_{cat} = 0.1$ g, $T = 373$ K, $P_{H_2} = 2.0$ MPa, $C_{IBAP} = 0.27$ mol/L, solvent *n*-decane. (b). Relative *4*-IBPE (solid symbols) and *4*-IBEB (open symbols) concentration as a function of time for different catalyst amounts. Reaction conditions: $T = 373$ K, $P_{H_2} = 2.0$ MPa, $C_{IBAP} = 0.27$ mol/L, solvent *n*-decane (a) 0.05 g of catalyst; (b) 0.1 g of catalyst; (c) 0.15 g of catalyst.

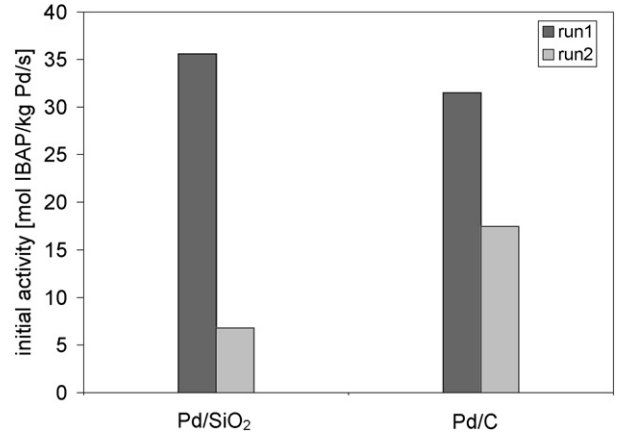

Fig. 5. Activity drop on successive runs during *4*-IBAP hydrogenation. Reaction conditions: $T = 373$ K, $P_{H_2} = 2.0$ MPa, $w_{cat} = 0.1$ g, $C_{IBAP} = 0.27$ mol/L, solvent *n*-decane.

compared with the value of about 50% reported in literature [2,3]; however, the *4*-IBPE yield passed through a maximum and appeared to be dependent on the amount of catalyst used (Fig. 4b). A drop in activity was observed when the reaction

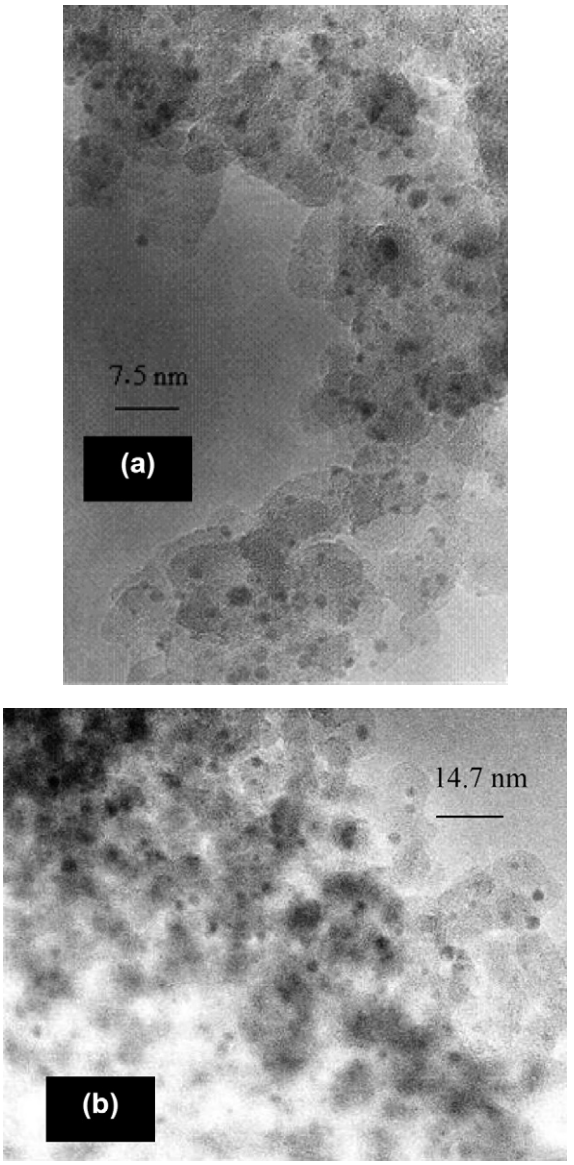

Fig. 6. TEM images of (a) fresh Pd/SiO_2; (b) spent Pd/SiO_2.

mixture along with the catalyst were held at the reaction temperature ($T = 373$ K) for an extended period (~12 h) and subsequently pressurized with H_2 (Fig. 2a), compared to when the reactor was immediately pressurized with H_2 on attaining the reaction temperature. The drop in initial activity on successive hydrogenation runs without catalyst treatment is shown in Fig. 5 for Pd/SiO_2 and Pd/C.

3.1. Catalyst characterization

The fresh and spent Pd/SiO_2 catalysts were characterized using TEM, N_2 physisorption and CO chemisorption. TEM studies on fresh Pd/SiO_2 revealed Pd crystallite sizes in the range of 0.5–3 nm (Fig. 6a). CO chemisorption studies on Pd/SiO_2 indicated an average Pd crystallite size of 3.5 nm (based on hemispherical geometry), confirming the TEM results. The Pd crystallite size increased slightly (to 4–5 nm) for the spent catalyst (Fig. 6b) compared with the fresh catalysts (Fig. 6a). CO

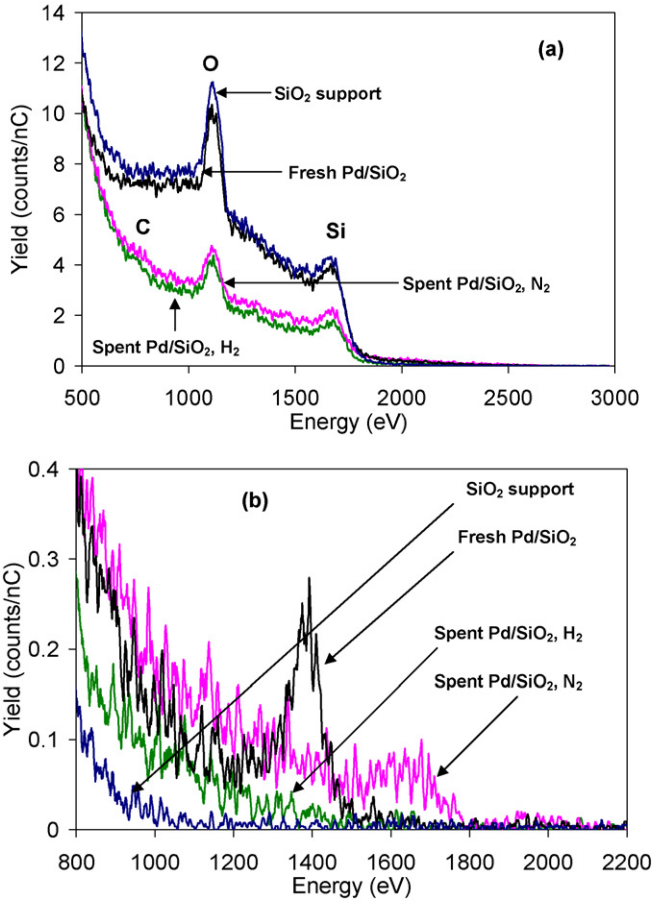

Fig. 7. (a) $^4He^+$ and (b) Ne^+ LEIS spectra for the 'as received' samples. Sample numbers indicated in the figure.

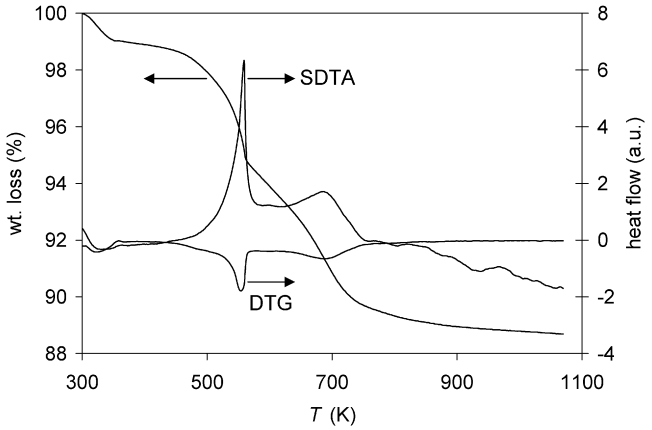

Fig. 8. TGA in air of spent Pd/SiO_2.

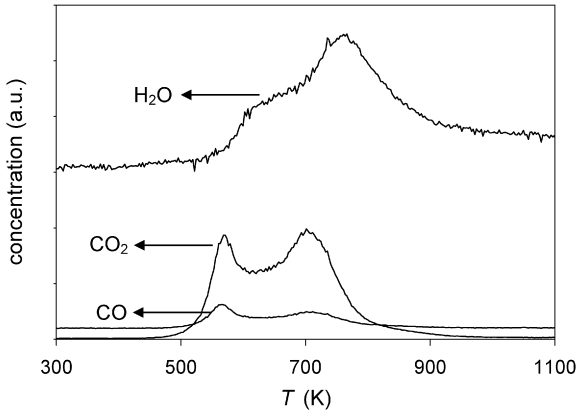

Fig. 9. TPO-MS of spent Pd/SiO_2.

chemisorption was also performed on a spent Pd/SiO_2 calcined at similar conditions ($T = 503$ K) as for the samples studied by LEIS, and also on a spent Pd/SiO_2 calcined at $T = 873$ K. The sample calcined at $T = 503$ K showed an apparent drop of 80% in Pd chemisorption capacity, which can be attributed to the presence of deposits on the Pd surface that block access of the CO probe molecules during chemisorption. The sample calcined at $T = 873$ K showed only a 30% drop in Pd chemisorption capacity. Calcining the sample at 873 K should be sufficient to oxidize all deposits on the catalyst surface, and the 30% drop in chemisorption capacity can be attributed to Pd sintering due to high-temperature calcination. N_2 physisorption also indicated an apparent drop of 12% in the specific SiO_2 surface area of the spent Pd/SiO_2.

Fig. 7 shows the results of analysis of all of the samples studied with the LEIS technique. Samples Pd/SiO_2, H_2 and Pd/SiO_2, N_2 contain organic carbonaceous deposits, as demonstrated by the small carbon peak corresponding to ∼750 eV and also by the lower intensities of O and Si compared with the fresh Pd/SiO_2 and the SiO_2 support, respectively (Fig. 7a). The Pd was also completely covered by deposits as seen in Fig. 7b. The Pd/SiO_2, N_2 showed the presence of an additional compound with atomic mass 141 corresponding to ∼1600 eV (Fig. 7b).

Fig. 8 shows the thermogravimetric analysis in air of the spent Pd/SiO_2. The spent catalyst was first calcined at 473 K for 1 h to desorb/burn the solvent and products adsorbed on it. Single-point differential thermal analysis (SDTA), along with the DTG, can determine whether the component desorbs from the sample or is burnt off. A peak on the SDTA profile corresponding to a trough on the DTG profile indicates the combustion of the component from the sample. An significant weight loss was observed at around 550 K, with another small one at around 700 K. Two DTG peaks were also observed in this temperature range.

Temperature-programmed oxidation coupled with mass spectrometry (TPO-MS) is a useful technique for characterizing the nature of species deposited on the catalyst surface. The TPO-MS profile of the spent Pd/SiO_2 is shown in Fig. 9. The catalyst sample was from the same batch of spent catalyst used for the TGA test. Three distinct profiles are observed in Fig. 9, corresponding to the evolution of CO, CO_2, and H_2O. The H_2O evolution peak is corrected for the H_2O evolved due to dehydroxylation of SiO_2 at elevated temperatures. The FTIR spectra of the fresh and spent Pd/SiO_2 are shown in Fig. 10. A sharp band observed at 3745 cm^{-1} indicates the presence of isolated silanol groups in the SiO_2 support [17]. The performance of Pd black during successive hydrogenation runs is shown in Fig. 11. The catalyst was dried at 373 K after the first run and charged to the reactor along with a fresh reaction mixture. Comparable

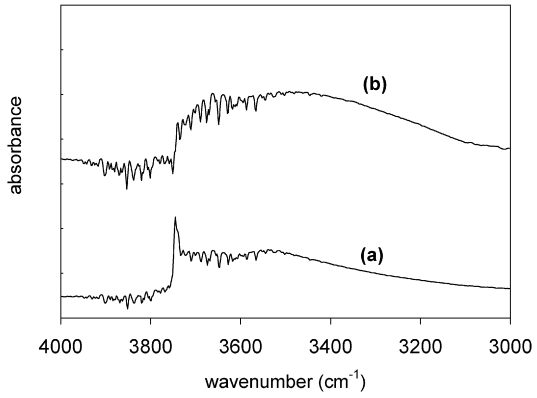

Fig. 10. FTIR spectra of (a) fresh Pd/SiO_2 and (b) spent Pd/SiO_2.

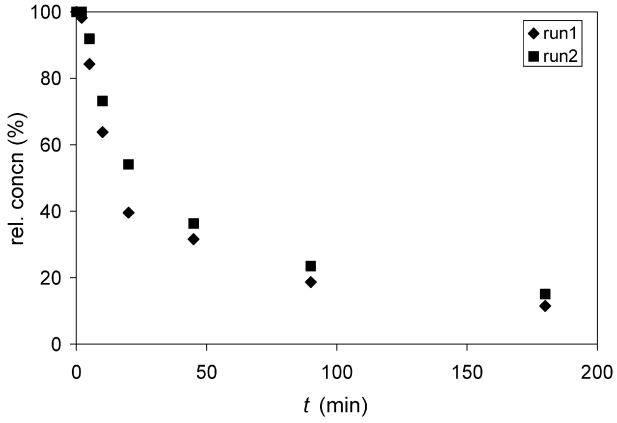

Fig. 11. Relative concentration versus time profile as a function of successive semi-batch runs using Pd black reaction conditions: w_{cat} (run 1) = 0.1 g, w_{cat} (run 2) = 0.075 g, $T = 373$ K, $P_{H_2} = 2.0$ MPa, $C_{IBAP} = 0.27$ mol/L.

conversion levels were observed in both runs, indicating that significant deactivation did not occur.

4. Discussion

4.1. Solvent and support effects

Because methanol is the most commonly used solvent for this reaction, we included it in the present study. Very low activity was observed. Although only low activity was observed when H_2O was used as a solvent (<5% conversion), moderate catalytic activity was still observed when H_2O was present (∼15 wt% with respect to *4*-IBAP) with *n*-decane as a solvent. Jaganathan et al. [18] observed a similar H_2O-inhibiting effect (also for H_2O concentrations >15 wt%) for the catalytic hydrogenation of *p*-nitrocumene over Pd/Al_2O_3, and Araya et al. [19] observed this effect during methane combustion over Pd/SiO_2. On replacing H_2O with a nonpolar solvent (*n*-decane), the hydrogenation of *4*-IBAP proceeded to full conversion.

The low activity observed on using excess H_2O (>15 wt%) might be due to the hydrophobicity of the organic substrates in a nonpolar reaction environment. At lower H_2O concentrations, H_2O may form a thin film around the SiO_2 due to cohesive interaction of H_2O with hydrophilic surface silanol groups, leading to agglomeration of the catalyst particles and, consequently, increased mass transfer resistance for the reactants [20]. Although no experiments were performed under controlled conditions to prove film formation, clusters of the catalyst particles in H_2O droplets were observed on opening the reactor after the reaction, demonstrating that water leads to agglomeration. The formation of *4*-iBuArC$(OH)_2CH_3$ by hydration of the ketone, which strongly binds to the Pd surface, preventing the attack of the hydride, also could explain the inhibiting effect of H_2O. Another advantage of using a nonpolar solvent is that the ether derivative of *4*-IBPE, an unwanted side product, which is usually formed in presence of methanol as a solvent [13], is eliminated by the use of *n*-decane.

Table 3
Solubility of hydrogen in solvents at reaction conditions

Solvent	Conditions	Solubility (mole fraction)	Reference
n-Decane	$T = 373$ K $P_{H_2} = 2.04$ MPa	2.04×10^{-2}	[30]
Cyclohexane	$T = 373$ K $P_{H_2} = 2.04$ MPa	1.12×10^{-2}	[31]

A slightly lower activity was achieved using cyclohexane as a solvent (Fig. 1). This can be attributed to the higher solubility of hydrogen in *n*-decane compared with cyclohexane (Table 3). The lower activity of $Pd/CaCO_3$ compared with the 2.4% Pd/SiO_2 catalyst (Fig. 2) could be attributed to the lower surface area of the $CaCO_3$ support (∼40 m^2/g), which has a negative impact on Pd dispersion and possibly also on the crystal structure.

The improved *4*-IBPE selectivity from using Pd/SiO_2 could be attributed to the small Pd crystallite size (0.5–3 nm). A drop in *4*-IBPE selectivity to 50% was observed on using Pd black, which had an average crystallite size of 74 nm.

4.2. Catalyst deactivation

The reaction profiles for *4*-IBAP hydrogenation (Fig. 4b) show a strong dependence on the catalyst loading, indicating that the catalyst probably deactivated during the course of reaction. Although this trend seems obvious for an intermediate product in a consecutive reaction, the leveling off of the *4*-IBEB profile when using a low catalyst concentration suggests that this behavior also can be attributed to catalyst deactivation. The possibility of the presence of feed poisons was excluded based on GC-MS and LEIS analysis. LEIS appears to be a very informative technique in this respect; it convincingly showed that neither the SiO_2 support nor the spent catalysts (Pd/SiO_2, H_2 and Pd/SiO_2, N_2) contained any traces of strongly adsorbing impurities. The impurity of atomic mass 141 (∼1600 eV), as seen in Fig. 7b, is attributed to Ce and can be explained by contamination of the spent catalyst (sample Pd/SiO_2, N_2) during calcination (before the LEIS analysis), because the same crucible had been used earlier for CeO_2 calcination. However, a severe drop (>80%) in hydrogenation activity was observed after the first run (Fig. 5). Rajashekharam et al. [13] also reported significant deactivation for the hydrogenation of *4*-IBAP with Ni/HY catalyst.

The possibility of polymerization of *4*-isobutylstyrene forming as an intermediate, leading to catalyst deactivation, can be excluded, because the C–O bond scission of *4*-IBPE occurred by direct hydrogenolysis [15]. Chang et al. [21] reported water poisoning for the selective hydrogenation of isoprene using Pd/δ-Al_2O_3. In our studies, water formed by the hydrogenolysis of *4*-IBPE could possibly deactivate the catalyst. Calcining the spent Pd/SiO_2 at 373 K in air restored only ∼50% of the original catalyst activity. Therefore, strong H_2O chemisorption was not the only reason for catalyst deactivation.

A common cause of catalyst deactivation is the formation of strongly adsorbing oligomeric/carbonaceous deposits from reactants or products due to undesired side reactions, leading to loss of activity by blocking the active sites [8]. For high-temperature gas-phase reactions in oil refineries, deactivation is usually associated with the formation of coke by a high degree of dehydrogenation; however for liquid-phase reactions at much lower reaction temperatures, deactivation due to oligomerization reactions is more probable [22–24]. Sometimes the activity can be recovered by removing the deposits with a suitable solvent; however, in the present study, washing the catalyst with pentane or acetone did not significantly improve the activity.

CO chemisorption studies on the spent Pd/SiO_2 indicated an apparent drop in Pd surface area from 3.4 m^2/g_{SiO_2} to only 0.3 m^2/g_{SiO_2}. In principle, the apparent loss of Pd surface area as measured by CO chemisorption could be attributed to oligomeric deposits covering the Pd surface, as well as to Pd crystallite growth. TEM analyses also reveal a slight increase in Pd crystallite size (Figs. 6a and 6b); however, obtaining a statistically representative TEM analysis can be difficult.

Two significant weight losses due to exothermic processes (SDTA) were observed on TGA of the spent catalyst (Fig. 8). A similar profile has been reported for Pt-reforming catalysts [25,26]. The first peak could be attributed to the combustion of organic deposits on the metal; the second peak, to the deposits on the support [27,28], as deduced from the exothermic peak in the SDTA profile. The TPO-MS profiles (Fig. 9) exhibit CO and CO_2 evolution at two distinct temperatures (∼550 and 700 K), in accordance with the TGA results. A 10% correction was made for the fragmentation of CO_2 to CO in the mass spectra. It is also interesting to note that H_2O evolved from 550 to 800 K, indicating that the deposits on the catalyst surface contain hydrogen. The TGA and TPO-MS analyses (Figs. 8 and 9) demonstrate that oligomeric deposits on the catalyst are at least partly responsible for the deactivation. These oligomers block the access of CO probe molecules on the Pd crystallites during CO chemisorption, which contributes to the apparent drop in calculated dispersion. The presence of C and the low intensity of Si on samples Pd/SiO_2, N_2 and Pd/SiO_2, H_2 (compared with the Si intensity of the SiO_2 support), as studied by LEIS (Fig. 7a), confirm the formation of oligomers, which also partly cover the SiO_2 support. This is also supported by reduction in the BET surface area of SiO_2. The low sensitivity of the LEIS instrument to C results in a very small, but significant, peak for C (Fig. 7a) [29].

The presence of isolated silanol groups that can impart local acidity to the SiO_2 support is shown in Fig. 10. Based on this observation, we propose that *4*-IBAP, an aromatic ketone, undergoes oligomerization by condensation-type reactions, thereby leading to the formation of higher-molecular weight species and subsequent catalyst deactivation, mainly by fouling. This mechanism also may explain the drop in catalyst activity, as shown in Fig. 2a. TGA of the spent SiO_2 sample subjected to a hydrogenation run under standard conditions ($w_{SiO_2} = 0.1$ g, $T = 373$ K, $C_{IBAP} = 0.27$ mol/L) showed a single exothermic peak (SDTA) ∼700 K, confirming the role of the SiO_2 support in oligomerization. The contribution of *4*-IBPE to oligomerization seems unlikely, because theoretically, a maximum of only two *4*-IBPE molecules can condense to form an ether, which might be insufficient to form oligomers. It was not possible to perform catalyst stability studies using *4*-IBPE, because the *4*-IBPE (in the absence of hydrogen atmosphere) was dehydrogenated to *4*-IBAP at the reaction temperature ($T = 373$ K) as observed by ATR-FTIR studies. Pressurizing the reactor with H_2 at room temperature itself would lead to the formation of *4*-IBEB at lower temperatures thus leading to erroneous results.

Since the oligomerization is proposed to occur due to the acidic nature of the isolated silanol groups on the Pd/SiO_2, the use of Pd black should not lead to any oligomerization/deactivation. A successive hydrogenation run performed using Pd black led to nearly similar conversion levels in both runs indicating that the deactivation was very modest (Fig. 11). This further confirms our proposition that the isolated silanol groups on the SiO_2 support led to oligomer formation. Calcining the spent Pd/SiO_2 at an extreme temperature of 873 K led to a 30% drop in the Pd surface area. Considering that the hydrogenations were performed at only 373 K, the contribution of Pd crystallite growth to catalyst deactivation must be insignificant compared with the contribution of oligomers.

To summarize, catalyst deactivation during *4*-IBAP hydrogenation over Pd/SiO_2 is proposed to occur due to the combined effects of (i) oligomerization of the reactant *4*-IBAP, (ii) strong H_2O inhibition, and (iii) Pd crystallite growth. The deactivation phenomenon was not restricted to the Pd/SiO_2 catalysts; it also was observed for commercial 5% Pd/C and 5% Pd/Al_2O_3 catalysts. This Pd/C contains relatively strong acid sites, explaining the deactivation by polymerization of the *4*-isobutylstyrene intermediate formed [15]. The alumina-supported catalyst was not analyzed in detail, but it is reasonable to assume that acid sites are present here as well. Deactivation was also observed over a 5% Pd/$CaCO_3$ catalyst, indicating that the deactivation phenomenon was not restricted to acidic supports only. Thus the deactivation due to oligomerization is an inherent feature of supported Pd catalyzed *4*-IBAP hydrogenation, irrespective of the type of support (acidic or basic) used.

5. Conclusion

Among the different supported Pd catalysts studied, Pd/SiO_2 showed the highest initial activity for hydrogenation of *4*-IBAP. The 80% yield of *4*-IBPE was significantly higher than that reported in the non-patented literature. The catalyst was significantly deactivated after a semibatch run, with no leaching of Pd

into the reaction medium. Characterization of the spent catalyst by a wide variety of techniques indicated that the formation of oligomers was one of the causes for the loss of catalytic activity. The presence of strongly adsorbing impurities leading to deactivation was excluded by LEIS analysis. Pd crystallite growth also was observed. H_2O was liberated during *4*-IBPE hydrogenolysis chemisorbed on the Pd, leading to loss of catalytic activity. The presence of isolated silanol groups resulted in increased acidity of the SiO_2 support, leading to the formation of oligomeric species on the catalyst surface and consequent deactivation.

Acknowledgments

This work was supported by the Netherlands Foundation for Technical Research (STW), Engelhard de Meern, and Quest International (project DPC 5772). The authors thank H.H. Brongersma and A. Knoester (Calipso B.V.) for the LEIS measurements and B. van der Linden (TUDelft) for assistance with the TPO-MS and IR setups.

References

[1] V. Elango, EP 0400 892 A2 (1990), to Hoechst–Celanese Corporation.
[2] S.P. Mathew, M.V. Rajashekharam, R.V. Chaudhari, Catal. Today 49 (1999) 49.
[3] M.V. Rajashekharam, R.V. Chaudhari, Chem. Eng. Sci. 51 (1996) 1663.
[4] H.U. Blaser, A. Indolese, A. Schnyder, H. Steiner, M. Studer, J. Mol. Catal. A 173 (2001) 3.
[5] G.F. Froment, Stud. Surf. Sci. Catal. 111 (1997) 53.
[6] J.A. Moulijn, A.E. van Diepen, F. Kapteijn, Appl. Catal. A 212 (2001) 3.
[7] C.H. Bartholomew, Appl. Catal. A 212 (2001) 17.
[8] P. Albers, J. Pietsch, S.F. Parker, J. Mol. Catal. A 173 (2001) 275.
[9] D.Y. Murzin, T. Salmi, Trends Chem. Eng. 8 (2003) 137.
[10] D.A. Ryan, EP 0358 420 A2 (1990), to Hoechst–Celanese Corporation.
[11] K. Saeki, K. Shima, JP 0262 837 (1990), to Daicel Chemical Ind. Ltd.
[12] V. Elango, EP 0400 892 A2 (1990), to Hoechst–Celanese Corporation.
[13] M.V. Rajashekharam, R.V. Chaudhari, Catal. Lett. 41 (1996) 171.
[14] J. Wang, B. McEnaney, Thermochim. Acta 190 (1991) 143.
[15] N. Thakar, N.F. Polder, K. Djanashvili, H. van Bekkum, F. Kapteijn, J.A. Moulijn, J. Catal. 246 (2007) 344.
[16] N. Thakar, R.J. Berger, F. Kapteijn, J.A. Moulijn, Chem. Eng. Sci. (2007) doi:10.1016/j.ces.2007.01.059.
[17] J.C. Groen, L.A.A. Peffer, J.A. Moulijn, J. Perez-Ramirez, Chem. Eur. J. 11 (2005) 4983.
[18] R. Jaganathan, V.G. Ghugikar, R.V. Gholap, R.V. Chaudhari, P.L. Mills, Ind. Eng. Chem. Res. 38 (1999) 4634.
[19] P. Araya, S. Guerrero, J. Robertson, F.J. Gracia, Appl. Catal. A 283 (2005) 225.
[20] B.M.A. Wolffenbuttel, T.A. Nijhuis, A. Stankiewicz, J.A. Moulijn, Catal. Today 69 (2001) 265.
[21] J.R. Chang, T.B. Lin, C.H. Cheng, Ind. Eng. Chem. Res. 36 (1997) 5096.
[22] E. Santacesaria, M. Di Serio, R. Velotti, U. Leone, Ind. Eng. Chem. Res. 33 (1994) 277.
[23] L.P. Tiainen, M.A. Paivi, A.K. Neyestenaki, T. Salmi, D.Y. Murzin, React. Kinet. Catal. Lett. 78 (2003) 251.
[24] M. Burgener, R. Wirz, T. Mallat, A. Baiker, J. Catal. 228 (2004) 152.
[25] C.L. Li, O. Novaro, E. Munoz, J.L. Boldu, X. Bokhimi, J.A. Wang, T. Lopez, R. Gomez, Appl. Catal. A 199 (2000) 211.
[26] J. Barbier, Appl. Catal. 23 (1986) 225.
[27] S.K. Sahoo, S.S. Ray, I.D. Singh, Appl. Catal. A 278 (2004) 83.
[28] W.J. Kim, E.W. Shin, J.H. Kang, S.H. Moon, Appl. Catal. A 251 (2003) 305.
[29] J.M.A. Harmsen, W.P.A. Jansen, J.H.B.J. Hoebink, J.C. Schouten, H.H. Brongersma, Catal. Lett. 74 (2001) 133.
[30] E. Brunner, J. Chem. Eng. Data 30 (1985) 269.
[31] M. Herskowitz, J. Wisniak, L. Skladman, J. Chem. Eng. Data 28 (1983) 164.